pp 1932–1942. © Royal Aeronautical Society 2016
doi: 10.1017/aer.2016.95

The influence of cavity's diamond pattern on the performance of gas dynamic lasers

A.M. Tahsini
a_m_tahsini@yahoo.com
Aerospace Research Institute
Tehran
Iran

ABSTRACT

The gas dynamic laser is numerically studied using quasi-1D and 2D simulations to investigate the effect of diamond pattern of the supersonic flow field (inhomogeneities in density field) on the laser's performance. The system of governing equations is solved with a finite volume approach using a structured grid in which the AUSM^{+} scheme is used to calculate the convective fluxes. Vibrational temperature of different modes, population inversion and the small signal gain are studied, and the effect of the divergent nozzle's geometry at the maximum gain is analysed.

Keywords: Diamond pattern; gain; gas dynamic; laser; nonequilibrium; numerical simulation; optical cavity; supersonic; vibrational energy

Received 11 July 2015; revised 5 April 2016; accepted 30 June 2016; first published online 8 September 2016.

NOMENCLATURE

A	lasing gas
a	constant in gain equation
B	gas stores the vibrational energy
b	constant in gain equation
C	catalyst gas
c	mass fraction
e	specific internal energy
e_{vib}	specific vibrational energy
h	enthalpy
h	Planck's constant
k	Boltzmann constant
N	population
p	pressure
R	gas constant
T	temperature
t	time
u	axial velocity
v	lateral velocity
X	mole fraction
x	axial coordinate
y	lateral coordinate
λ	wavelength
ρ	density
$\tau_{I,II}$	characteristic relaxation time of vibrational modes
τ_{12}	radiative lifetime
$v_{1,2,3}$	vibrational mode's frequency of gas A
v_c	collision frequency

Subscripts

I, II	vibrational modes
vib	vibrational

Superscripts

eq	equilibrium

1.0 INTRODUCTION

The usefulness of lasers in human life is undeniable. Laser technology is used in many research, medical, industrial, military, and commercial applications. There are different types of lasers with a wide range of wavelengths and powers, such as solid-state lasers or

https://doi.org/10.1017/aer.2016.95 Published online by Cambridge University Press

semiconductor lasers. Gas lasers are one of the most useful types and can be divided into three categories: electric discharge, chemical and gas dynamic lasers.

The invention of Gas Dynamic Lasers (GDLs) dates back about 50 years. The population inversions in molecular systems could be created by rapid heating or cooling of the system. Therefore, such inversions could be obtained in the rapid nonequilibrium expansion of an initially hot gas through a supersonic nozzle. During such expansions, the gas is turned into a supersonic laser medium and passes into the optical cavity, where using the mirrors may extract a beam of laser perpendicular to the flow. The revolutionary aspect of GDLs is that they can be scaled to large sizes without major physical complications. GDLs can produce maximum continuous wave powers up to hundreds of kilowatts[1].

Hurle and Hertzberg[2] proposed the practical idea of the GDL but were unsuccessful in their experiment. Kantrowitz et al[3] operated the first gas dynamic laser at the Avco Everett Research Laboratory in 1966. Several studies have been done on the GDLs in the past decades, which are summarized here.

Anderson[4] has numerically analysed the nonequilibrium flow in the GDL using a quasi-1D assumption and studied the temporal variation of the vibrational temperature along the nozzle. He also predicted the population inversion using this procedure[5]. Anderson et al[6] experimentally measured the laser gain and compared those data with their aforementioned numerical predictions. Christiansen and Tsongas[7] and Biriukov et al[8] experimentally investigated the effect of gas composition and chamber pressure on the gain parameter. McLeary[9] numerically studied the effect of stagnation temperature on the performance of the gas dynamic laser using quasi-1D simulation. Reddy[10,11] has also computed the effect of gas composition and nozzle area ratio on the gain parameter of GDL. He also used the same quasi-1D simulations.

The theoretical analysis of the gas dynamic laser is based on the consecutive computation of the vibrational temperatures, population inversions, gain and power extraction. Such calculations generally provide results on the raw power output available from the optical cavity, but the total picture of power extraction is more than that[12]. One reason for this difference is the density inhomogeneities of the flowing gas in the cavity that cause phase distortions in the laser beam. Such inhomogeneities are due to the diamond pattern of supersonic field due to the flow geometry interactions.

Investigating these 2D phenomena cannot be performed by quick 1D simulations. Some multi-dimensional simulations have been done on chemical gas lasers[13-15] and mixing layer gas dynamic lasers[16], but there is no concentrated study of the diamond pattern effects on the performance of the conventional GDLs. In the present work, the variation of the gas dynamic laser's gain along the optical cavity is numerically investigated using 2D calculations to analyse the effects of the flow field's diamond pattern.

2.0 GOVERNING EQUATIONS AND NUMERICAL PROCEDURE

In the present study, the laser mixture contains the A–B–C gas mixture in which A is the active lasing molecule, B stores the vibrational energy and C has the role of catalyst for augmentation of the population inversions. The 2D compressible equations governing the continuum inviscid flow representing the conservation of mass, momentum, and energy are used as the basic equations of the flow field. These equations are written in the following

https://doi.org/10.1017/aer.2016.95 Published online by Cambridge University Press

conservation form[17].

$$\frac{\partial U}{\partial t}+\frac{\partial F}{\partial x}+\frac{\partial G}{\partial y}=0, \quad \ldots(1)$$

where

$$U=\begin{bmatrix}\rho\\ \rho u\\ \rho v\\ \rho e\end{bmatrix} \quad F=\begin{bmatrix}\rho u\\ \rho uu+p\\ \rho uv\\ \rho uh\end{bmatrix} \quad G=\begin{bmatrix}\rho v\\ \rho vu\\ \rho vv+p\\ \rho vh\end{bmatrix} \quad \ldots(2)$$

The laser media under consideration has two modes of vibrational energy, so:

$$e=e(T)+\frac{V^2}{2}+e_{vibI}+e_{vibII} \quad \ldots(3)$$

The rate equations representing the relaxation of vibrational energies of these modes are:

$$\begin{aligned}\frac{\partial e_{vibI}}{\partial t}+u\frac{\partial e_{vibI}}{\partial x}+v\frac{\partial e_{vibI}}{\partial y}&=\frac{1}{\tau_I}\left(e_{vibI}{}^{eq}-e_{vibI}\right)\\ \frac{\partial e_{vibII}}{\partial t}+u\frac{\partial e_{vibII}}{\partial x}+v\frac{\partial e_{vibII}}{\partial y}&=\frac{1}{\tau_{II}}\left(e_{vibII}{}^{eq}-e_{vibII}\right)\end{aligned} \quad \ldots(4)$$

For the CO_2–N_2–H_2O or the N_2O–N_2–He mixtures as A–B–C system, the vibrational energies are defined as:

$$\begin{aligned}e_{vibI}&=c_A R_A\left\{\left(\frac{h\upsilon_1}{k}\right)\left[exp\left(\frac{h\upsilon_1}{kT_{vibI}}\right)-1\right]^{-1}+\left(\frac{2h\upsilon_2}{k}\right)\left[exp\left(\frac{h\upsilon_2}{kT_{vibI}}\right)-1\right]^{-1}\right\}\\ e_{vibII}&=c_A R_A\left\{\left(\frac{h\upsilon_3}{k}\right)\left[exp\left(\frac{h\upsilon_3}{kT_{vibII}}\right)-1\right]^{-1}\right\}\end{aligned} \quad \ldots(5)$$

The populations of two energy levels of the lasing molecule are:

$$\begin{aligned}N_{001}&=\frac{N_A exp\left(-\frac{h\upsilon_3}{kT_{vibII}}\right)}{\left[1-exp\left(-\frac{h\upsilon_1}{kT_{vibI}}\right)\right]^{-1}\left[1-exp\left(-\frac{h\upsilon_2}{kT_{vibI}}\right)\right]^{-2}\left[1-exp\left(-\frac{h\upsilon_3}{kT_{vibII}}\right)\right]^{-1}}\\ N_{100}&=\frac{N_A exp\left(-\frac{h\upsilon_1}{kT_{vibI}}\right)}{\left[1-exp\left(-\frac{h\upsilon_1}{kT_{vibI}}\right)\right]^{-1}\left[1-exp\left(-\frac{h\upsilon_2}{kT_{vibI}}\right)\right]^{-2}\left[1-exp\left(-\frac{h\upsilon_3}{kT_{vibII}}\right)\right]^{-1}}\end{aligned} \quad \ldots(6)$$

Finally, these populations are used to compute the small signal gain using the relation:

$$G_o=\left(\frac{\lambda^2}{4\pi\tau_{12}\upsilon_c}\right)(N_{001}-N_{100})\left(\frac{a}{T}\right)exp\left(-\frac{b}{T}\right) \quad \ldots(7)$$

https://doi.org/10.1017/aer.2016.95 Published online by Cambridge University Press

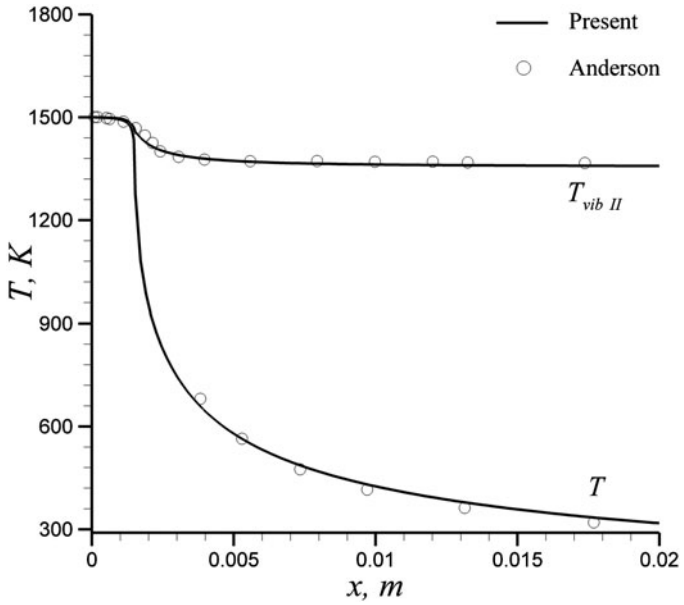

Figure 1. Vibrational and translational temperature distribution.

The parameters in these equations are defined in the nomenclature. Here, the cell-centred finite volume method used to discretise the six governing equations is defined. All equations are coupled and are discretized on structured grids. The time integration is accomplished by an explicit time stepping scheme[18]. The flux terms are treated using an AUSM$^+$ method (Advection Upstream Splitting Method) at cell faces[19]. The local time steps are used to speed up the computations and obtain the final steady state results.

The developed numerical procedure has been validated and used in different flow fields[20-22]. In addition, to show the validity of this code for the considered problem, two different GDLs are considered. At first, the CO_2–N_2–H_2O flow of Ref. 5 is solved in convergent-divergent nozzle geometry to compare the distribution of the vibrational temperature as shown in Fig. 1. Then, the N_2O–N_2–He gas dynamic laser[10] is calculated to compare the small signal gain distribution as illustrated in Fig. 2. The results show the accuracy of the present numerical simulation program.

Since the results of the mentioned references have been calculated using quasi-1D method, for comparison, the present 2D code is reduced and converted to 1D form. To do this, the lateral momentum equation is omitted and the effect of area change is entered as a source term in an axial momentum equation[23].

3.0 RESULTS AND DISCUSSION

The gas dynamic laser is the converging-diverging nozzle which is continued by the constant area chamber as an optical cavity (laser resonator). The gas dynamics of such supersonic flow field in this cavity may contain some expansion and compression waves, which make the diamond pattern there. This pattern causes the flow's inhomogeneities, which are improper for the laser beam. The presence of the diamond pattern and its influence must be studied using

https://doi.org/10.1017/aer.2016.95 Published online by Cambridge University Press

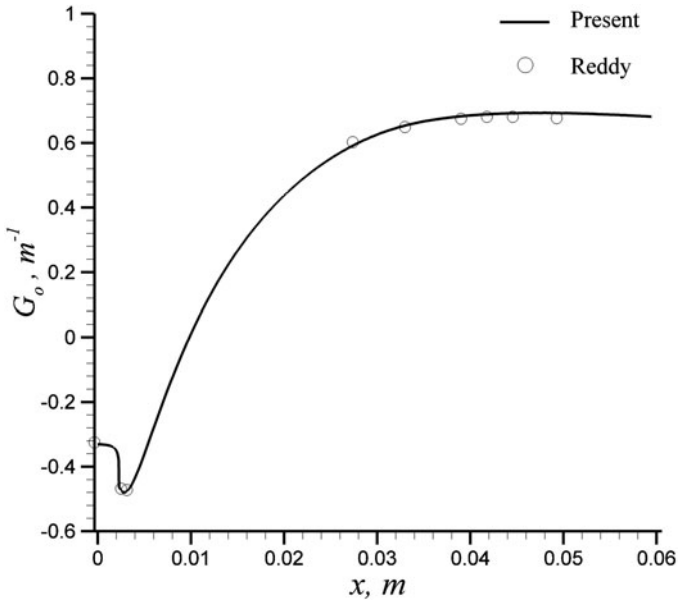

Figure 2. Small signal gain distribution.

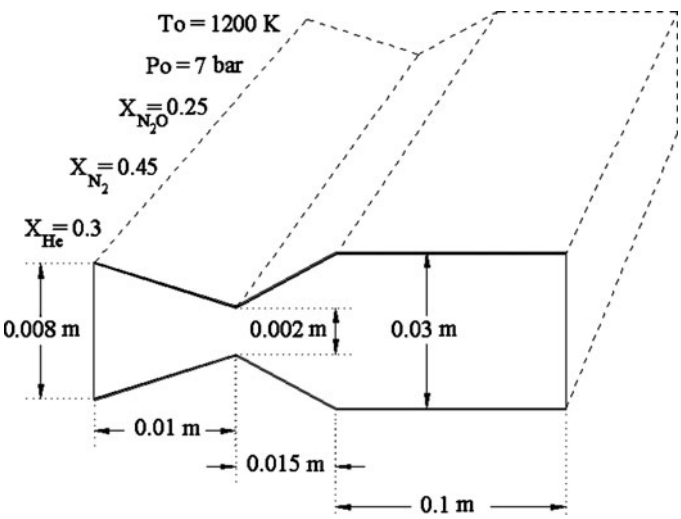

Figure 3. Geometry and flow properties of the considered GDL.

2D simulations. The GDL considered here is N_2O–N_2–He laser with geometry (not scale) and flow properties as shown schematically in Fig. 3. The inlet condition is $T_o = 1{,}200K$, $p_o = 7\ bar$, $X_{N2O} = 0.25$, $X_{N2} = 0.45$ and $X_{He} = 0.3$. The outlet flow is supersonic and the outlet boundary condition is extrapolated from the inside. The divergent part has three different geometries: linear, quarter of cosine function, and half of cosine-function. The grid resolution of 150×50 is chosen here after the grid independency studies. The 2D simulations last about 2 hours on the core-i7 2.8 GHz CPU PC.

https://doi.org/10.1017/aer.2016.95 Published online by Cambridge University Press

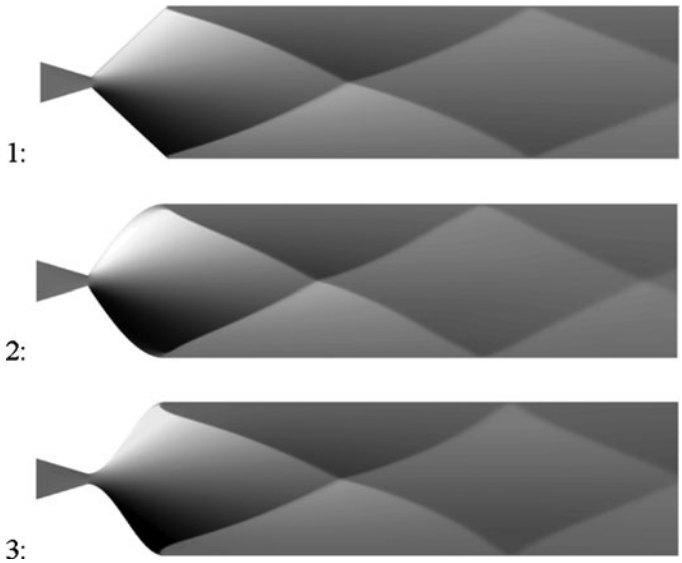

Figure 4. Lateral velocity contours for different geometries of divergent nozzle.

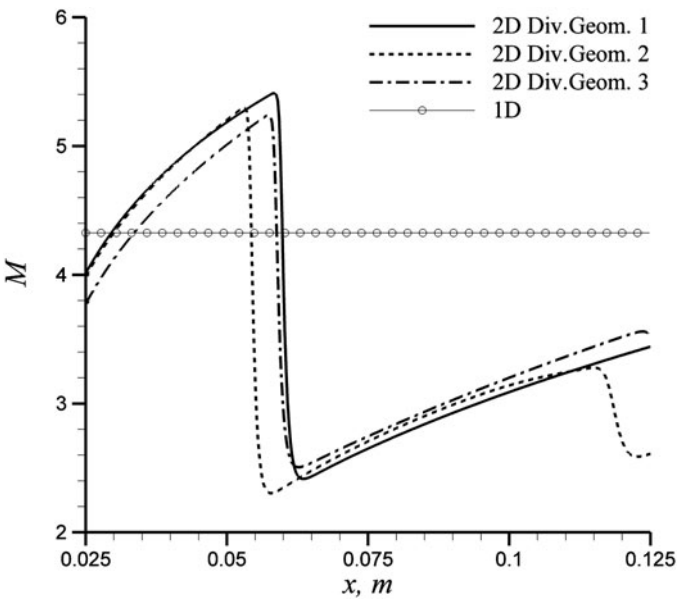

Figure 5. Mach number distribution along the cavity's centreline.

The results of the flow field simulation (without considering the vibrational energies) are shown in Fig. 4, which illustrates the diamond pattern in the supersonic region. The geometry of the divergent nozzle has some impacts on flow field but apart from that, there are many differences between the 2D and quasi-1D simulations as shown in Figs 5 and 6. Temperature and Mach number distributions along the cavity's centreline (in a straight channel after divergent nozzle) indicate the effect of the diamond pattern as about 50% deviation in Mach

https://doi.org/10.1017/aer.2016.95 Published online by Cambridge University Press

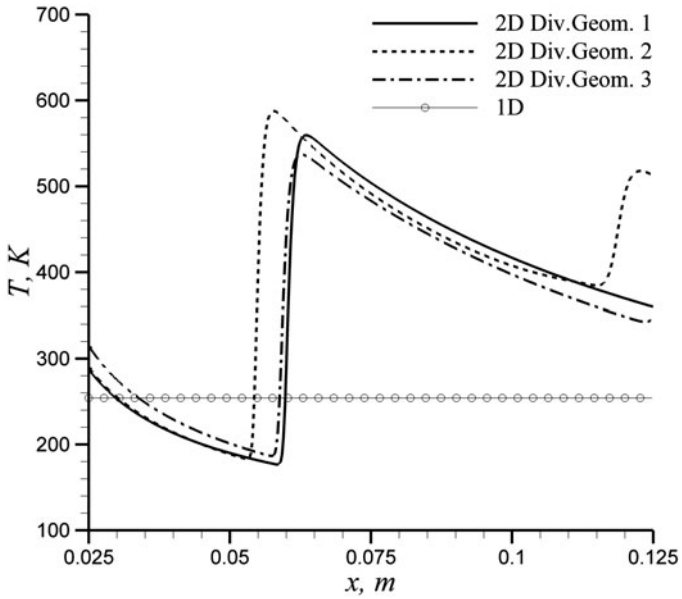

Figure 6. Temperature distribution along the cavity's centreline.

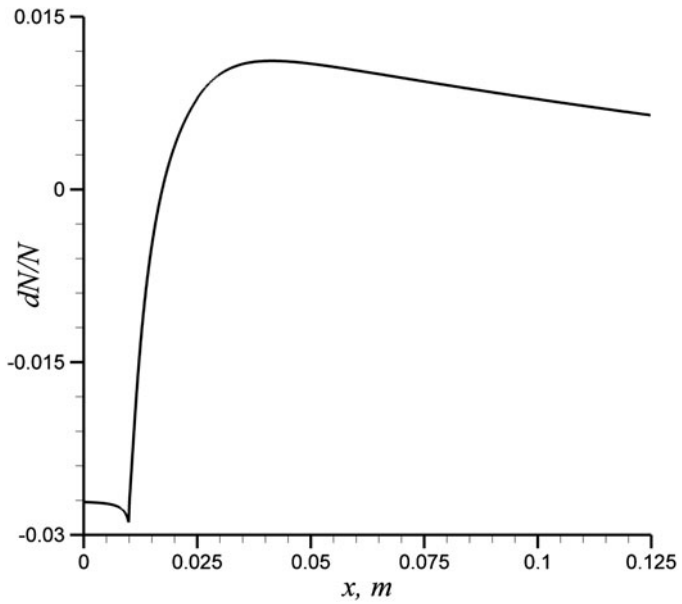

Figure 7. Distribution of population inversion from quasi 1D simulation.

number and 140% deviation in temperature at some places in the optical cavity. Such 2D phenomena alter the performance of the GDL, as will be illustrated.

Taking into account the equations for vibrational energy modes helps to compute the population inversions and small signal gain of the GDL. The distribution of the population inversion is shown in Fig. 7 using the quasi-1D simulation, which indicates that the maximum

https://doi.org/10.1017/aer.2016.95 Published online by Cambridge University Press

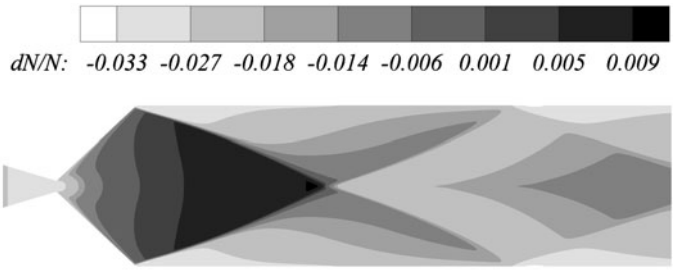

Figure 8. Population inversion contours for the first geometry.

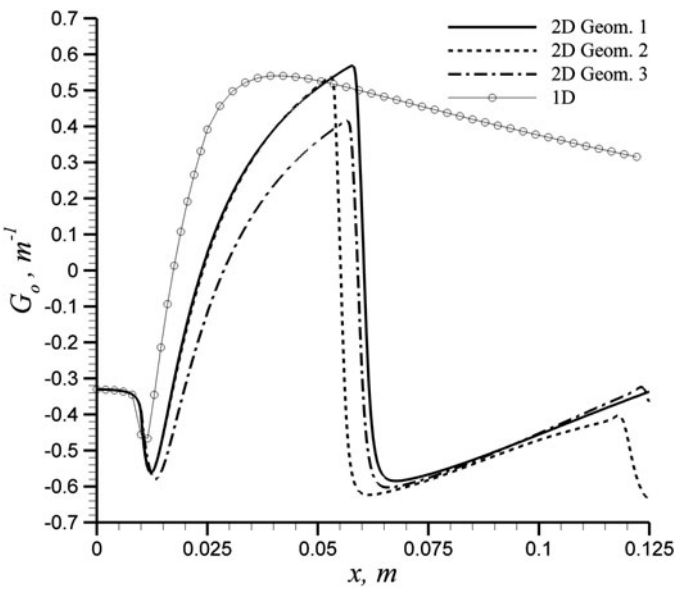

Figure 9. Distribution of small signal gain along the centreline.

inversion occurs at the initial sections of the cavity and is about 0.011. The 2D result for the first configuration is shown in Fig. 8. The maximum inversion decreases slightly due to the 2D effects and occurs at a position downstream of the 1D simulation.

The small signal gain and the second mode's vibrational temperature are also compared in Figs 9 and 10, respectively. The results indicate that the maximum gain depends to the geometry of the divergent nozzle, and its position is downstream of the results of the 1D computation. The maximum gain growth is about 40% between different geometries. The diamond pattern drastically decreases the population inversions and the small signal gain along the cavity. Compression waves (oblique shock waves) slow down the supersonic flow in the cavity and increase the resident time, so the nonequilibrium effects are weakened.

4.0 CONCLUSION

Numerical study of the gas dynamic laser is performed here by quasi-1D and 2D simulations. The results show the influences of the 2D pattern of the supersonic flow field in an optical

https://doi.org/10.1017/aer.2016.95 Published online by Cambridge University Press

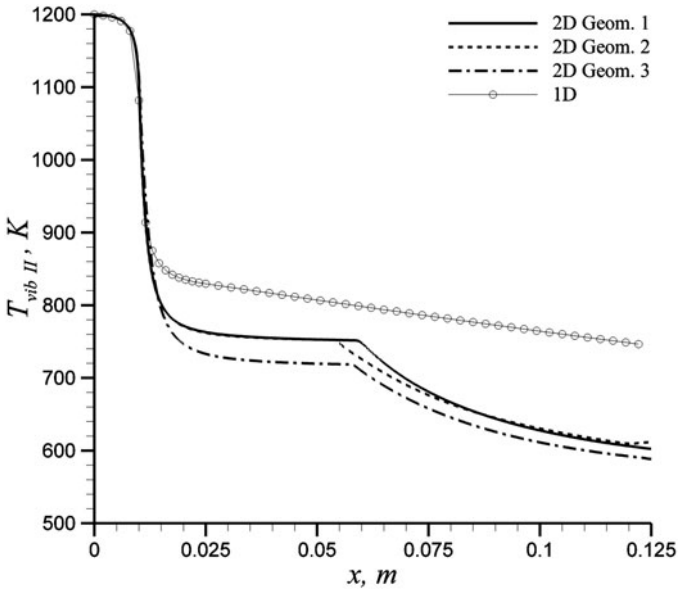

Figure 10. Distribution of the second mode's vibrational temperature along the centreline.

cavity on the laser's performance. Such behaviour cannot be analysed using 1D computation. The maximum small signal gain occurs in the centreline and at the position downstream of the 1D result, and the compression waves collision decreases drastically the small signal gain. The existence of a diamond pattern in the optical cavity may increase the resident time and attenuate the nonequilibrium effects at the cavity's downstream. The geometry of the divergent nozzle has an important effect on the maximum gain due to the alteration of the diamond pattern. Here, the maximum gain variation is about 40% due to the geometry. The results indicate that the 2D simulations must be used for design and optimization of gas dynamic lasers.

REFERENCES

1. ENDO, M. and WALTER, R.F. *Gas Lasers*, 1st ed., 2007, CRC Press, Taylor & Francis Group, Florida, US.
2. HURLE, I.R. and HERTZBERG, A. Electronic population inversions by fluid-mechanical techniques, *Physics of Fluids*, 1965, **8**, (9), pp 1958-1988.
3. GERRY, E.T. Gasdynamic lasers, *IEEE Spectrum*, 1970, **7**, (11), pp 51-58.
4. ANDERSON, J.D. A time-dependent analysis for vibrational and chemical nonequilibrium nozzle flows, *AIAA J.*, 1970, **8**, (3), pp 545-550.
5. ANDERSON, J.D. Time-dependent analysis of population inversions in an expanding gas, *Physics of Fluids*, 1970, **13**, (8), pp 1983-1989.
6. ANDERSON, J.D., HUMPHREY, R.L., VAMOS, J.S., PLUMMER, M.J. and JENSEN, R.E. Population inversions in an expanding gas: Theory and experiments, *Physics of Fluids*, 1971, **14**, (12), pp 2620-2624.
7. CHRISTIANSEN, W.H. and TSONGAS, G.A. Gain kinetics of CO_2 gasdynamic laser mixtures at high pressure, *Physics of Fluids*, 1971, **14**, (12), pp 2610-2619.
8. BIRIUKOV, A.S., DRONOV, A.P., KOUDRIAVTSEV, E.M. and SOBOLEV, N.N. Gas dynamic CO_2-He-(N_2) laser investigations, *IEEE J. Quantum Electronics*, 1971, **7**, (8), pp 388-391.

https://doi.org/10.1017/aer.2016.95 Published online by Cambridge University Press

9. MCLEARY, R. Calculation of gain and power output for a gas-dynamic laser, *IEEE J. Quantum Electronics*, 1972, **8**, (8), pp 716-718.
10. REDDY, K.P.J. Time-dependent analysis of an N_2O gasdynamic laser, *AIAA J.*, 1989, **27**, (10), pp 1387-1391.
11. REDDY, N.M. and REDDY, K.P.J. Theoretical gain optimization studies in 16-micron CO_2-N_2-H_2 gasdynamic lasers, *AIAA J.*, 1985, **23**, (6), pp 883-888.
12. ANDERSON, J.D. *Gasdynamic Lasers: An Introduction*, 1st ed., 1976, Academic Press, New York, US.
13. HU, Z., JIANG, Z., MYONG, R. and CHO, T. Numerical analysis of spatial evolution of the small signal gain in a chemical oxygen-iodine laser operating without primary buffer gas, *Optics & Laser Technology*, 2008, **40**, pp 13-20.
14. PARK, J.S., BAEK, S.W. and BYUN, D. Variation of population inversion and gain characteristics with D2 injection angle in DF chemical laser cavity, *Int. J. Heat and Mass Transfer*, 2008, **51**, pp 361-377.
15. PARK, J.S. and BAEK, S.W. Numerical study of base effects on population inversion in DF chemical laser cavity, *Int. J. Heat and Mass Transfer*, 2006, **49**, pp 4043-4057.
16. CHAKRAVARTY, P., REDDY, N.M. and REDDY, K.P.J. Two-dimensional analysis of a 16-micron CO_2 downstream-mixing gasdynamic laser, *AIAA J*, 1987, **25**, (5), pp 713-720.
17. KUO, K.K. *Principles of Combustion*, 2nd ed., 2005, Wiley and Sons, Hoboken, New Jersey, US.
18. HIRSCH, C. *Numerical Computation of Internal and External Flows*, 1988, Wiley and Sons, Hoboken, New Jersey, US.
19. LIOU, M.S. A sequel to AUSM: $AUSM^+$, *J. Computational Physics*, 1996, **129**, pp 364-382.
20. TAHSINI, A.M. Heat release effects on drag reduction in high speed flows, *Int. J. Heat and Mass Transfer*, 2013, **57**, (2), pp 657-661.
21. TAHSINI, A.M. and TADAYON MOUSAVI, S. Investigating the supersonic combustion efficiency for the jet-in-cross-flow, *Int. J. Hydrogen Energy*, 2015, **40**, (7), pp 3091-3097.
22. TAHSINI, A.M. Turbulence and additive effects on ignition delay in supersonic combustion, *IMechE J. Aerospace Engineering*, 2013, **227**, (1), pp 93-99.
23. TAHSINI, A.M. Non-steady burning effect on solid rocket motor performance, 45th AIAA Aerospace Sciences Meeting and Exhibit, Aerospace Sciences Meetings, 2007, Reno, Nevada, US.

https://doi.org/10.1017/aer.2016.95 Published online by Cambridge University Press